SCIENCE CHINA
Earth Sciences

•ARTICLE•

March 2024 Vol.67 No.3: 657–672
https://doi.org/10.1007/s11430-023-1258-4

The genesis and resource potential of gold deposits in the Liaodong Peninsula

Rixiang ZHU[1*], Jin-Hui YANG[1], Gongwen WANG[2], Qingdong ZENG[1], Guoqiang XUE[1], Tao XU[1], Xinghui LI[1], Peng ZHANG[3], Da LEI[1] & Guang ZHU[4]

[1] *State Key Laboratory of Lithospheric Evolution, Institute of Geology and Geophysics, Chinese Academy of Sciences, Beijing 100029, China;*
[2] *School of Earth Sciences and Resources, China University of Geosciences, Beijing 100083, China;*
[3] *Shenyang Center, China Geological Survey, Shenyang 110034, China;*
[4] *School of Resources and Environmental Engineering, Hefei University of Technology, Hefei 230009, China*

Received October 24, 2023; revised December 13, 2023; accepted January 17, 2024; published online February 26, 2024

Abstract Plenty of gold deposits related to Late Mesozoic craton destruction are widely distributed in eastern North China Craton. However, significant differences in research degrees, ore-forming characteristics, and proven reserves exist among different regions in the North China Craton. The Liaodong Peninsula has similar regional geological characteristics to those of the Jiaodong Peninsula, with both experiencing craton destruction during Late Mesozoic, but the two areas have substantial differences in terms of gold mineralization and the proven gold resources. Based on regional geology, Mesozoic magmatic-tectonic evolution and ore geology, combined with integrated geophysical exploration and big data AI resource prediction, in this paper, we propose that the ore-forming materials of Late Mesozoic gold deposits in Liaodong were mainly originated from mantle-derived melts and/or fluids induced by craton destruction. The gold deposits were primarily controlled by NE-NNE-trending faults, mainly classified as fracture-controlled altered rock-type and sulfide-bearing quartz vein-type. Moreover, our study predicts that the Yalu River fault zone and its related secondary faults, as well as the periphery and deeper parts of known goldfields, are the important regions for future gold resource exploration. The Yalu River metallogenic belt has an enormous potential for gold resources, and the Liaodong Peninsula has a potential to add thousands of tons of gold resources.

Keywords Liaodong Peninsula, Gold deposit, Integrated geophysical exploration, Prospecting potential, Direction for prospecting breakthroughs

Citation: Zhu R, Yang J, Wang G, Zeng Q, Xue G, Xu T, Li X, Zhang P, Lei D, Zhu G. 2024. The genesis and resource potential of gold deposits in the Liaodong Peninsula. Science China Earth Sciences, 67(3): 657–672, https://doi.org/10.1007/s11430-023-1258-4

1. Introduction

Globally, super-large gold deposits are predominantly distributed in old cratons, and are associated with orogeny and metamorphism during cratonization, commonly referred to as orogenic gold deposits (Goldfarb et al., 2001). The gold precipitates at shallow crustal depths from gold-enriched H_2O-CO_2 fluid derived from dehydration, desulfurization, and decarbonation during greenschist- to amphibolite-facies prograde metamorphism at mid-crustal depths, migrating to shallower crustal levels and precipitating (Gebre-Mariam et al., 1995; Phillips and Powell, 2010; Tomkins, 2010; Yu et al., 2024). The North China Craton contains widely distributed large to super-large Mesozoic gold deposits, and its proved reserves account for more than 50% of the national total. The host rocks for these deposits are Precambrian metamorphic rocks and Mesozoic magmatic intrusions. Groves et al. (1998) considered the Jiaodong gold deposits as orogenic gold deposits. However, recent studies indicate that the Jiaodong area experienced multiple tectonic events, in-

* Corresponding author (email: rxzhu@mail.iggcas.ac.cn)

cluding late Paleozoic subduction of the Paleo-Tethys Ocean, early Mesozoic continental collision, and Late Mesozoic craton destruction (Zhang et al., 1988; Zheng et al., 2018; Zheng et al., 2019). The gold deposits in the Jiaodong and other regions of the eastern North China Craton mainly formed in the Early Cretaceous, coeval to the emplacement of lamprophyre and diabase dykes in the same areas under an extensional environment associated with Cretaceous lithospheric thinning and asthenospheric upwelling (Sun and Shi, 1995; Yang et al., 2003; Mao et al., 2005, 2008). The gold mineralization was related to tectonism, magmatism, and fluid activities induced by craton destruction deduced by the subduction of the ancient Pacific Plate. They are distinct from orogenic gold deposits in terms of ore-forming fluids, sources of materials, depository geology, and ore-forming background (Zhu et al., 2015, 2020; Wu et al., 2019; Mao et al., 2021; Yang et al., 2021 and references therein). Thus, some scholars argue that the gold deposits in North China are not orogenic in origin but "the Jiaodong-type gold deposits" (Deng et al., 2015, 2023) or "Decratonic gold deposits" (Zhu et al., 2015). Recently, Mao et al. (2021) investigated the characteristics and tectonic background of polymetallic mineralization along the eastern edge of the Eurasian continent, and proposed that the Cretaceous gold deposits in Jiaodong and Liaodong are part of large-scale mineralization in the post-subduction extensional environment of the late Pacific Plate, with ore-forming elements derived from deep lithospheric dynamic processes.

Gold deposits in different parts of the eastern North China Craton vary significantly in research depths, mineralization types, geological characteristics, and proven reserves. The Jiaodong area has proven gold reserves of over 5400 tons (Deng et al., 2020a; Yu et al., 2024), accounting for more than one-third of the national total. The Liaodong area, located to the east of the Tan-Lu fault, has similar Precambrian basement rocks and widespread Mesozoic magmatic rocks to the Jiaodong area, and also experienced the similar craton destruction processes. However, the discovered gold resources in Liaodong are significantly less than those in Jiaodong. To deeply study the genesis of gold deposits in Liaodong and to find strategic replacement base of gold resources, the Chinese government has recently set up special projects for multidisciplinary comprehensive research in geology, geochemistry, and geophysics of the gold deposits in Liaodong (Mao et al., 2005; Yang et al., 2021; Di et al., 2021; Wang G et al., 2021). These studies further indicate the potential of huge gold resources in the Liaodong area, with proven gold reserves approaching a thousand tons. This paper proposes new directions for future research and gold prospecting in Liaodong, based on comparative analysis of the deep lithospheric structure, Mesozoic tectonic evolution, Mesozoic magmatism and geodynamics, and large-scale gold mineralization in the Jiaodong and Liaodong regions.

2. Late Mesozoic geology of the Liaodong area

The Liaodong area, located in the northeastern part of the North China Craton, lies between the Tan-Lu fault zone and the Yalu River fault zone, bordering the Central Asian Orogenic Belt (also known as the Xing-Meng Orogenic Belt) in the north (Figure 1). To the south of the Bohai Sea, the Jiao-Bei Uplift in the southeastern margin of the North China Craton develops with large-scale Early Cretaceous decratonic/Jiaodong-type gold deposits (Zhu et al., 2015; Deng et al., 2015, 2023). During the basement evolutionary stage, the main body of Liaodong belonged to the ancient Proterozoic Jiao-Liao-Ji Orogenic Belt. The Longgang Block is located to the northwest of the Haicheng-Benxi South-Tonghua in its northwest Liaodong and the Langlin Block is located to east of the Yalu River Fault Zone in its east part (Zhang S et al., 2017). The exposed rocks in Liaodong include Archean to Paleoproterozoic metamorphic basement rocks, covered by Mesoproterozoic to Paleozoic marine sedimentary rocks, locally with Jurassic to Cretaceous continental volcanic-sedimentary rocks and a series of Mesozoic intrusions.

During the peak destruction period of the North China Craton (Zhu R X et al., 2011, 2012; Wu et al., 2019; Yang et al., 2021; Zhu G et al., 2021), widespread and intensive magmatism and crustal extension with the development of a series of extensional structures occurred in the Liaodong area (Zhu G et al., 2021 and references therein). In recent years, a large amount of high-precision isotopic data have shown that the Mesozoic magmatic rocks in Liaodong can be divided into three periods: Triassic (231–200 Ma), Jurassic (183–152 Ma), and Early Cretaceous (131–120 Ma), of which the Early Cretaceous granites and volcanics are the most widespread (Wu et al., 2005a; Yang and Wu, 2009; Sun et al., 2021). Triassic magmatic rocks mainly include alkaline rocks and calc-alkaline gabbro-diorite-granite (Yang et al., 2012; Zhu Y S et al., 2017), and Jurassic magmatic rocks are primarily intermediate-felsic diorite-granodiorite-granite, with rare mafic rocks (Wu et al., 2005b; Sun et al., 2021), whereas the Early Cretaceous magmatic rocks are complex in rock types, including alkaline rocks, A-type granites, I-type granites, and widely associated intermediate-mafic rocks (Yang et al., 2021). In terms of their emplacement age and rock types, the Mesozoic magmatic rocks in the Liaodong area are generally similar to those in the Jiaodong area. The most intensive magmatism occurred in the Early Cretaceous during the peak destruction period of the North China Craton (Figure 1b) under a strong extensional setting.

Early Cretaceous extensional structures are widespread, including a series of metamorphic core complexes, detachment faults, high-angle normal faults, layer-parallel extensional sliding fracture zones, and extensional basins in the Liaodong Peninsula (Figure 1b). Exposed in the southern part of Liaodong are the Liaonan and Wanfu metamorphic

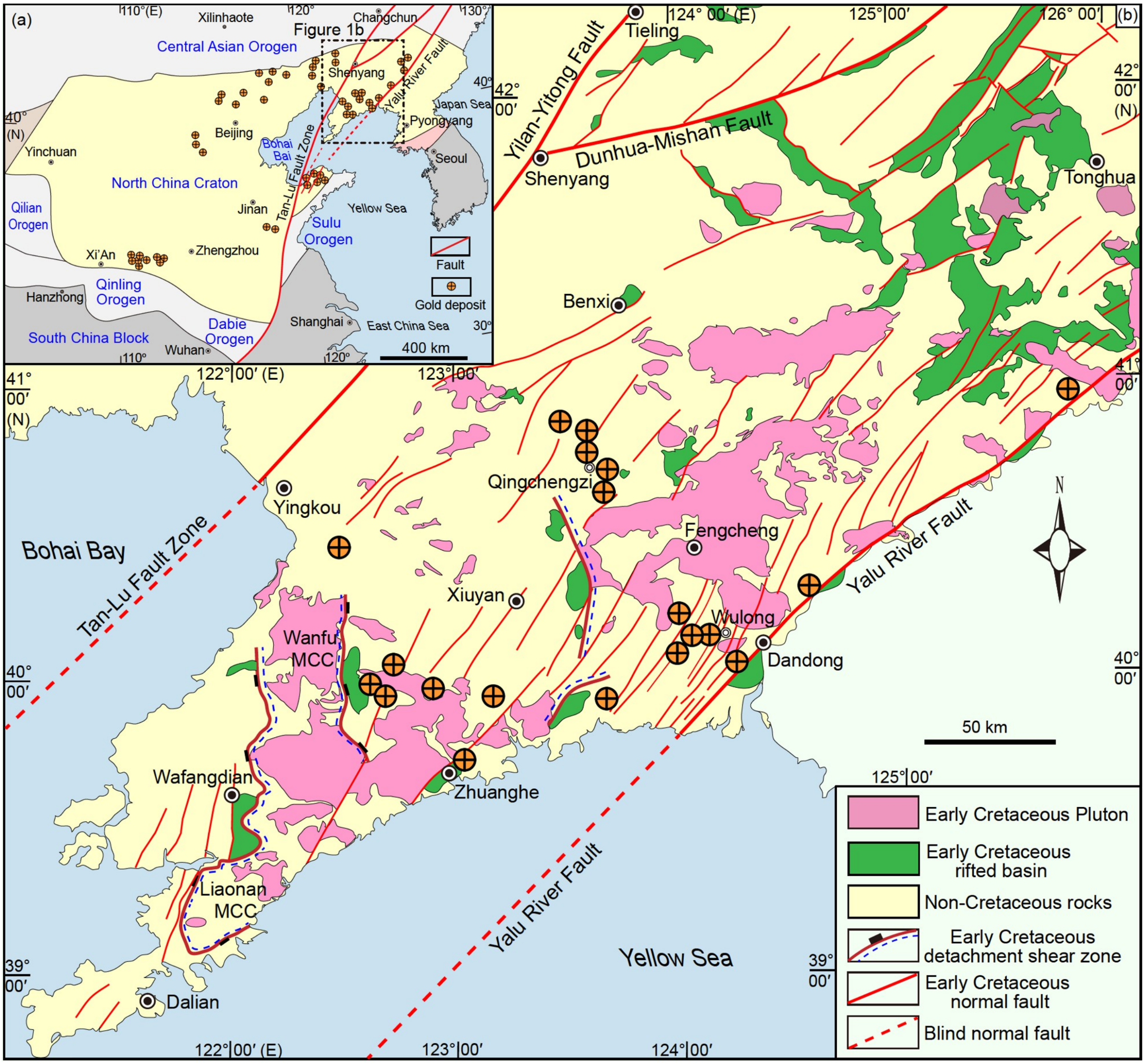

Figure 1 Simply geological map showing the distributions of gold deposits in the eastern North China Craton (a) and the distribution of Early Cretaceous extensional structures, magmatic rocks, and gold deposits in the Liaodong peninsula (b).

core complexes (Lin et al., 2008; Liu et al., 2013), the cores of which are Archean metamorphic rocks and Mesozoic intrusions that were originally located at mid-crustal levels. Overlying these metamorphic core complexes are Mesoproterozoic to Paleozoic marine covers, and the detachment fault zones control the development of Early Cretaceous superimposed basins. The Liaonan and Wanfu metamorphic core complexes had experienced rapid uplift and exhumation during 120–110 Ma (Yang et al., 2007; Lin et al., 2011). The Dayingzi and Gushan low-angle detachment fault zones developed to the west of the Wanfu metamorphic core complex, with an overlying extensional basin on the upper plate (Liu et al., 2011). Early Cretaceous NE-SW trending high-angle normal faults are widespread in the central and northern parts of the Liaodong area, and they were newly formed, generally smaller on scale, and reactivated earlier left-lateral strike-slip faults, including the giant Tan-Lu and Yalu River fault zones (Zhu G et al., 2012, 2018; Zhang et al., 2018, 2019). Early Cretaceous layer-parallel extensional sliding fracture zones, mainly developing at the contact zone between the Proterozoic Dashiqiao Formation marbles of Liaohe Group and the overlying Xianxian Group schists, are low-angle and are characterized by the development of breccia zones commonly with dikes and mineralization. This type of extensional structure mainly developed in the Qingchengzi goldfield in central Liaodong with predominantly NE-trending (Zeng et al., 2019).

A series of Early Cretaceous extensional basins developing in the Liaodong area are all small-scale volcanic-sedimentary basins (Liu et al., 2011; Yan et al., 2021), and can be divided into three types: superimposed basins developing in the upper plate of the detachment fault zones of the Liaonan and Wanfu metamorphic core complex (i.e., eastern Guiyunhua Basin, western Pulandian-Wafangdian Basin); extensional basins in the upper plate of the Dayingzi and Gushan low-angle detachment fault zones (i.e., Huanghuaxun-Dayingzi Basin and Gushan Basin); and fault-bounded basins controlled by high-angle normal faults (such as the Dandong Basin and Tongyuanbao Basin; Zhang et al., 2019). ^{40}Ar/^{39}Ar dating of a series of extensional ductile detachment shear zones in Liaodong, along with zircon U-Pb dating of volcanic rocks within the extensional basins, constrain the Early Cretaceous extensional activity at 135–106 Ma (Yang et al., 2007; Lin et al., 2008, 2011; Liu et al., 2011, 2013; Zhang et al., 2019, 2020; Yan et al., 2021). During Early Cretaceous time, the Yalu River fault zone transformed into a large-scale normal fault with the eastern block subsiding, and controlled the development of a series of rift basins (Zhang et al., 2019); the western block was an uplifted block, exposing the upper crust and accompanying a series of NE-SW trending high-angle normal faults (Zhang S et al., 2020).

3. Geophysical exploration and deep-shallow lithospheric structures

3.1 Deep lithospheric structure in the Liaodong Peninsula

Based on investigations on regional geology and gold deposits in the Liaodong peninsula, mobile seismic array detection was deployed across the Wulong and Qingchengzi goldfields with SE-trending, and shallow integrated geophysical exploration of these goldfields was conducted to reveal the deep structure of the regional lithosphere and the shallow structure and hidden plutonic bodies in the two ore fields (Figure 2a). Integrating data from the northeastern margin of the North China Craton and adjacent regions′ broadband mobile arrays (NCISP6 and NCISP10) and fixed stations (Meng et al., 2021; Ma et al., 2022), Zhang et al. (2014) and Meng et al. (2021) used teleseismic S-wave receiver function migration imaging to obtain the depth variation of Liaodong lithosphere (Figure 2b). As shown in Figure 2b, the AA′ profile crossing the Wulong and Qingchengzi goldfields shows that the lithospheric thickness increases from about 65 km in the east to around 100 km in the southern part of the Da Hinggan Mountains. This indicates that the lithosphere in the Liaodong area has been strongly destructed and thinned with spatial heterogeneity, and it becomes significantly thinner along the Tan-Lu and the Yalu River fault zones, and there are also obvious thermal anomalies under the lithosphere, indicating that deep faults play an important role in the process of craton destruction and lithospheric thinning, which provides a channel for deep molten fluid to penetrate upward. The significant thinning of lithosphere thickness and the strong metasomatism of molten fluid may be one of the important factors of the Late Mesozoic gold mineralization in Liaodong (Figure 2b). Figure 2c reveals the top surface of the Archean basement about 5 km beneath the Longgang Block, possibly extending eastward into the Jiao-Liao-Ji Orogenic Belt and gradually deepening, which was disrupted by the boundary fault between the Longgang Block and the Jiao-Liao-Ji Orogenic Belt (BLJ). Previous research indicates that the lithosphere beneath the Jiaodong area had been significantly thinned (Chen, 2010; Zhu et al., 2011). All of these observations indicate that both the Liaodong and Jiaodong areas share a common structure and dynamic background of lithospheric destruction and thinning.

3.2 Shallow geophysical exploration and geological structures in the goldfields

To reveal the shallow crustal structures and ore-controlling structures of the Wulong and Qingchengzi goldfields in Liaodong, ground-based geo-electric, airborne transient electromagnetic, airborne magnetic, and short-period seismic array investigations were conducted. The geophysical explorations have revealed magnetic, electrical, and velocity anomalies in the Wulong and Qingchengzi goldfields (Di et al., 2020; Xie et al., 2021; Zheng et al., 2022). Previous ground magnetic data show strong magnetism in the magnetite quartzite of the Liaohe Group and weak magnetism in its marble, schist, and granulite. The Mesozoic granites in the area are weakly magnetic, the gabbro is moderately magnetic, and the non-mineralized quartz veins are weakly magnetic or non-magnetic, while mineralized quartz veins containing pyrrhotite are slightly more magnetic (Di et al., 2020). The interpretations of magnetic anomalies in the goldfields are summarized as follows.

(i) Wulong goldfield. After processing the aeromagnetic anomalies, it was found that the magnetic field in the detection area all show NE-trending, characterized by high values in the northwest and low values in the southeast (Figure 3a). To the northwest of the central part of the observed area, marked by the NE section of the Jixinling fault, is a large high magnetic anomaly area, while the southeast part shows a negative anomaly. The NE-oriented magnetic anomaly strips basically align with the positions of the Hongshi, Yangjia, and Jixinling faults, all characterized by stable, continuous magnetic anomalies.

Aeromagnetic data well constrain the boundaries and lithologies of geological bodies. Area B in Figure 3a represents the non-magnetic or weakly magnetic Liaohe Group strata, likely comprising marble, schist, and granulite, while Area A represents the high-magnetic anomaly area of the

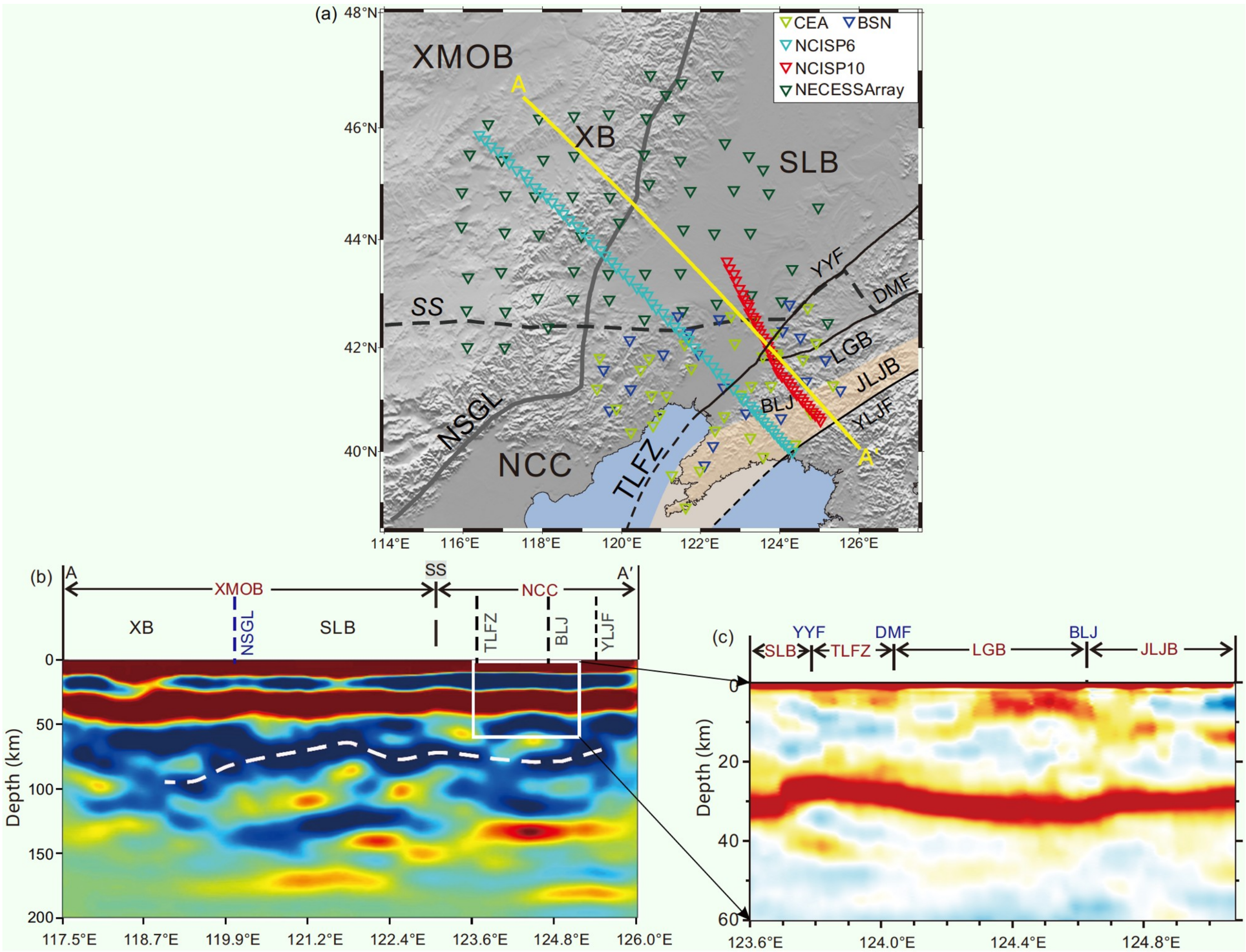

Figure 2 Lithospheric structures in Liaodong. (a) Location of the AA′ profile; (b) Lithospheric thickness on the AA′ profile (modified from Zhang et al., 2014; Meng et al., 2021); (c) Crustal structure in the area marked by the white square in Figure 2b (modified from Dong et al., 2022). XMOB, Xing-Meng Orogenic Belt; NCC, North China Craton; XB, Xing'an Block; SLB, Songliao Basin; TLFZ, Tan-Lu Fault Zone; YLJF, Yalu River Fault Zone; NSGL, North-South Gravity Gradient Zone; SS, Suolun Suture Zone; YYF, Yilan-Yitong Fault; DMF, Dunhua-Mishan Fault; LGB, Longgang Block; JLJB, Jiao-Liao-Ji Orogenic Belt; BLJ, Boundary between the Longgang block and Jiao-Liao-Ji orogenic belt.

Liaohe Group containing magnetite particles (Figure 3a). The semicircular low magnetic anomaly in the southeastern part of the detection area corresponds to the exposure locations of Sanguliu intrusion (Figure 3a, Area C). The Wulong intrusion exhibits weak magnetism, but a high magnetic anomaly appears in the northwest of the detection area, speculated to be related to the deep Liaohe Group metamorphic rocks and later mafic intrusions. The central part of the detection area shows a moderate magnetic anomaly, presumably related to the exposed gneissic biotite monzogranite and two-mica monzogranite of the Wulong intrusion.

To understand the distribution of electrical properties at different depths, resistivity cross-sections at the surface, 100 meters, and 300 meters depth were drawn based on airborne transient electromagnetic data (Figure 3b). Within 300 meters depth, the electrical distribution in the detection area is basically consistent with resistivity showing a clear high in the north and low in the south, and low-resistivity zones distributed at equal intervals from NE to SW. Aeromagnetic data reflect the boundaries and lithologies of intrusions consistent with aeromagnetic detection results (Figure 3a). Areas A and B are both Liaohe Group strata, overall showing low resistivity characteristics, Area C shows high resistivity, corresponding to the exposure locations of the Sanguliu intrusion, whereas the other area is the Wulong intrusion, mainly exhibiting high-resistivity characteristics. Due to tectonic effects, the electrical distribution of the Wulong intrusion is uneven, with some areas showing medium resistivity characteristics.

(ii) Qingchengzi goldfield. Four intrusions (B, D, C, E) are exposed in the Qingchengzi goldfield (Figure 4a). The Middle to Late Triassic monzogranite intrusion (D) exhibits high magnetism, while the Proterozoic monzogranite intrusions (B, C, E) show medium to low magnetism. A high magnetic zone (Area A) near the Yaojia molybdenum deposit is proposed to be a mineralized Middle Jurassic granite in-

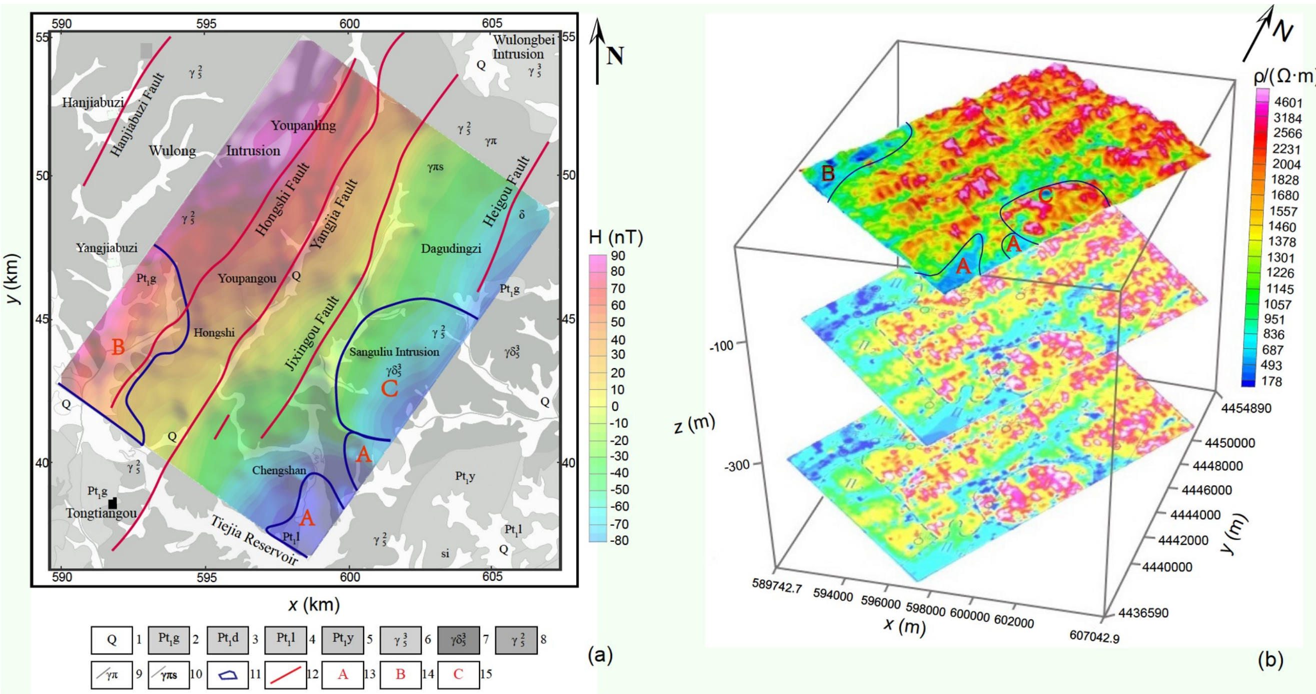

Figure 3 Aeromagnetic and aeroelectric results of the Wulong goldfield. (a) Aeromagnetic anomaly interpretation plan. 1, Quaternary; 2, Proterozoic Liaohe Group Gaixian Formation; 3, Proterozoic Liaohe Group Dashiqiao Formation, third member; 4, Proterozoic Liaohe Group Langzishan Formation; 5, Proterozoic Liaohe Group Yujiapuzi Formation; 6, Triassic granite dikes; 7, Triassic granodiorite dikes; 8, Jurassic granitedikes; 9, Granitic porphyry dikes; 10, Altered granitic porphyry; 11, Intrusion boundary; 12, Faults; 13, Liaohe Group formations (Gaixian and Dashiqiao formations); 14, Liaohe Group formations (Langzishan and Yujiapuzi formations); 15, Sanguliu intrusion. (b) 3D inversion resistivity slices of airborne transient electromagnetic data at different depths.

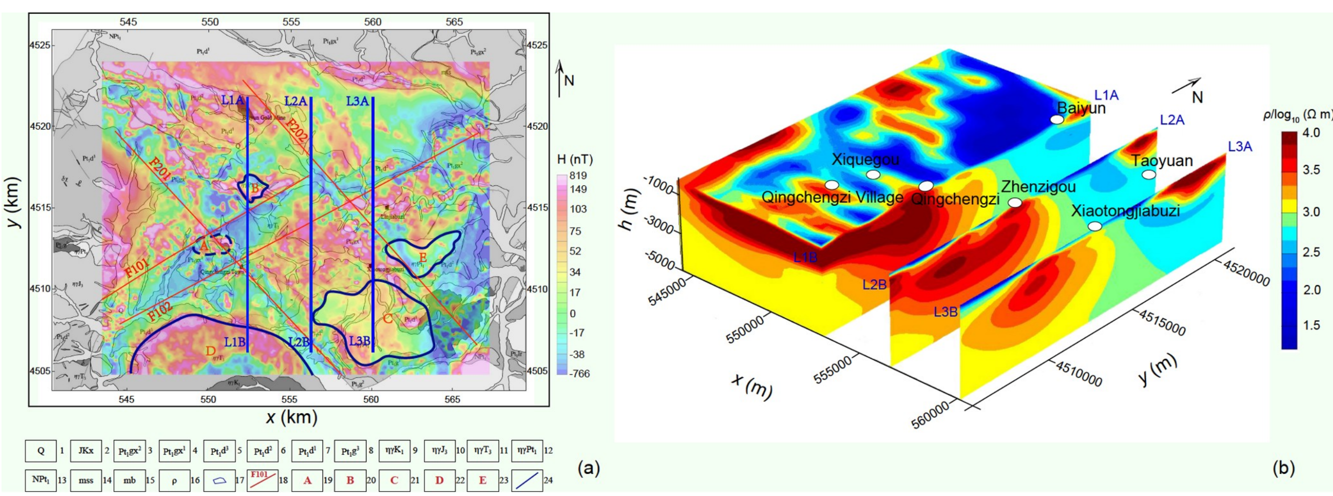

Figure 4 Planar map of aeromagnetic anomaly and magnetotelluric resistivity map in the Qingchengzi goldfield. (a) Planar map of aeromagnetic anomaly. 1, Quaternary; 2, Jurassic-Cretaceous Xiaoling Formation; 3, Second segment of the Proterozoic Gaixian Formation, Liaohe Group; 4, first segment of the Proterozoic Gaixian Formation, Liaohe Group; 5, third segment of the Proterozoic Dashiqiao Formation, Liaohe Group; 6, second segment of the Proterozoic Dashiqiao Formation, Liaohe Group; 7, first segment of the Proterozoic Dashiqiao Formation, Liaohe Group; 8, Proterozoic Gaojiayu Formation, Liaohe Group; 9, Early Cretaceous monzogranite; 10, Late Jurassic monzogranite; 11, Late Triassic monzogranite; 12, Proterozoic monzogranite; 13, Neoproterozoic strata; 14, Metamorphic sandstone; 15, Marble; 16, Pegmatite vein; 17, Intrusion boundary; 18, Faults; 19, Yaojiagou intrusion; 20, Xinling intrusion; 21, Dadingzi intrusion; 22, Shuangdinggou intrusion; 23, Nanshan intrusion; 24, Detection line number. (b) 3D magnetotelluric inversion resistivity slice map.

trusion.

Aeromagnetic data confirm the development of two groups of faults in the area, i.e., NE- (F101 and F102) and NW-trending (F201 and F202) faults (Figure 4a), revealing the extension of these two fault groups at depths in their respective directions. The F101 fault in the central-southern part of the goldfield has a length of 14 km within the detection area. Its northern side shows a stronger magnetic field, while the southern side shows a weaker one, with molybdenum deposits located at its intersection and controlled by the F201 fault. The F102 fault occurs approximately 28 km in length in the area, with a weak positive magnetic field on the southern side and a weak negative magnetic field on the northern side, indicating lithological differences on either side of the fault.

The 3D magnetotelluric sounding method obtained underground electrical data to a depth of 5 km (Figure 4b), showing high resistivity near the surface in the L1 A, L2 A, and L3 A line profiles (Figure 4a and 4b), which is presumed to be exposed or hidden granite. Low resistivity areas are presumed to be the Proterozoic Gaixian Formation strata of the Liaohe Group. Several famous polymetallic deposits in the area are close to faults and are mostly located in the weak positive/negative magnetic field gradient zones (Figure 4b). The area near Xiaotongjiapuzi (Figure 4b, Line L3) is located in a high to low resistivity transition zone and extends deeply. Short-period seismic array noise imaging reveals a hidden intrusion possibly existing down to 5 km beneath Xiaotongjiapuzi (Xie et al., 2021), speculated to be the gold mineralization zone (Di et al., 2020).

4. Genesis of gold deposits in the Liaodong Peninsula

4.1 Mineralization age of Liaodong gold deposits

In the Liaodong Peninsula, gold deposits primarily consist of quartz vein type and altered rock type. Recent advances have been made in determining the mineralization ages of these deposits. In the Wulong gold deposit, various dating methods yielded consistent mineralization ages, including molybdenite Re-Os isochron age of 125±2 Ma for gold-bearing quartz veins, hydrothermal monazite SIMS U-Pb age of 127±3 Ma (Yu et al., 2020), hydrothermal rutile SIMS U-Pb age of 122±1 Ma (Feng et al., 2020), and sericite $^{40}Ar/^{39}Ar$ age of 123±1 Ma (Liu et al., 2019). These ages are consistent with those of the spatially associated intermediate-mafic dikes in the goldfield, indicating coeval Early Cretaceous mineralization and magmatism. Controversy has long surrounded the mineralization age of the Qingchengzi goldfield. Based on the cross-cutting relationships between orebodies and dikes and their zircon U-Pb ages, Sun et al. (2019, 2020, 2022) proposed that the gold deposits in the area were formed mainly in the Early Cretaceous (~126 Ma). Controversy has also surrounded the timing of the mineralization of the Maoling goldfield in western Liaodong, ranging from Paleoproterozoic (2316±140 Ma, Yu et al., 2005; 2287±95 Ma, Liu et al., 2018), through the early Jurassic (~189±5 Ma, Zhang P et al., 2017), to early Cretaceous (~129 Ma, Liu et al., 2018) (Liu et al., 2018). Significant breakthroughs have been made in recent exploration in the Dadonggou gold deposit, which also has an Early Cretaceous mineralization age. The Xinfang gold deposit in the south of the Yalu River fault zone has a pyrite Re-Os isochron age of 121±1 Ma (Zhang et al., 2022) and a sulfide Rb-Sr isochron age of 123±2 Ma (Zhang et al., 2023). The ages of pre-and post-mineralization dikes in the Xindian gold deposit are 127 Ma and 121 Ma, respectively, constraining an Early Cretaceous mineralization age (Yu et al., 2018, 2020, 2022). Hydrothermal monazite from gold-bearing quartz veins of the Gulouzi gold deposit in the central part has an U-Pb age of 121±7 Ma (unpublished data by the author). The Shawogou gold deposit in the north formed between 126–129 Ma (unpublished data by the author). All of these data show that the main mineralization of gold deposits in the Liaodong area occurred in the Early Cretaceous, which is consistent with that of the Jiaodong gold deposits.

4.2 Ore-controlling structures of Liaodong gold deposits

The ore-controlling structures in the Liaodong area are predominantly high-angle normal faults with NE-trending and low-angle, layer-parallel extensional sliding fracture zones with nearly EW-trending (Xiao et al., 2018; Zeng et al., 2019). Quartz vein-type gold deposits are primarily controlled by high-angle normal faults, while altered rock-type gold deposits are controlled by both high-angle normal faults and low-angle, layer-parallel extensional sliding fracture zones. The well-explored Wulong gold deposit, a quartz vein-type gold deposit, is primarily controlled by high-angle NE-trending normal faults and their associated structures (Xiao et al., 2018), which include newly-formed normal faults during the Early Cretaceous extension period as well as reactivated early left-lateral strike-slip faults and their derivative faults (Zhang S et al., 2020). The host rock for orebodies is the Late Jurassic Wulong monzogranite intrusion. The Sidaogou gold deposit in the south of the Yalu River fault zone and the Maoling gold deposit in central Liaodong are altered rock-type gold deposits, developing within the Paleoproterozoic Liaohe Group. The ore-hosting structure in the Sidaogou gold deposit is the interlayer fracture zone of the Liaohe Group, with the orebodies oriented NE and NW, while the Maoling gold deposit is situated in the fracture zone of high-angle normal faults. In the Qingchengzi goldfield, altered rock-type gold deposits, including the Baiyun, Xiaotongjiapuzi, Taoyuan, and Linjia Sandaogou deposits, are controlled by low-angle, layer-parallel extensional sliding fracture zones with EW-trending (Zeng et al., 2019), mainly developing within the Dashiqiao Formation marble and Gaixian Formation schist of the Liaohe Group. They are characterized by multi-phase activities, initially as reverse thrust-overlapping interlayer sliding zones (Zhang S H et al., 2020) and later transforming into extensional interlayer sliding zones (Zeng et al., 2019). Extensive alteration of the wall rocks occurred in each type of gold deposit, with a clear pattern of hydrothermal alteration zoning. From the vein center to the wall rocks, it can be sequentially divided into pyrite sericitization (silicification) - sericitization (chloritization) - unaltered rock.

Gold deposits in the Liaodong area occur as clusters within specific zones and belts. Based on their clustered distribution, they are divided into the Qingchengzi polymetallic field, the Maoling goldfield, and the Yalu River gold metallogenic belt (Figure 1). The Yalu River metallogenic belt extends NE along the eastern side of the Liaodong Peninsula, bordering North Korea, and contains quartz vein-type gold deposits represented by the Wulong gold deposit and altered rock-type gold deposits represented by the Sidaogou and Dadonggou gold deposits. Quartz vein-type gold deposits were controlled by steeply NE-dipping faults, while altered rock-type gold deposits were controlled by interlayer faults of the Liaohe Group (Figure 5). Thus, gold mineralization in Liaodong was mainly controlled by NE-NNE trending faults, very similar to the ore-controlling structural patterns of the Jiaodong gold deposits (Figure 1). Gold mineralization in both Liaodong and Jiaodong occurred within a short period under similar tectonic setting, with the types of gold deposits primarily being altered rock-type in fracture zones and sulfide-bearing quartz vein-type.

4.3 Comparison of gold mineralization between Liaodong and Jiaodong

The Jiaodong Peninsula is one of China's most significant gold-producing areas, with over 5400 tons of gold resources identified within an area that constitutes only 0.17% of China's landmass, making it the world-wide third-largest gold mining district. The Liaodong and Jiaodong regions are fundamentally similar in terms of deep lithospheric structure, Mesozoic tectonic evolution, basement rocks, and magmatic rocks, especially characterized by the wide development of Early Cretaceous granites closely related to gold mineralization. The gold deposits in both regions have the same mineralization ages and characteristics (Miao et al., 1997; Yang et al., 2005; Jiang et al., 2010; Zhu et al., 2015; Goldfarb and Groves, 2015; Fan et al., 2021; Deng et al., 2022). Available studies using sulfide Rb-Sr isotopic dating methods (Yang and Zhou, 2001) and SHRIMP/LA-ICPMS U-Pb dating of hydrothermal zircon and monazite in quartz-sulfide veins have precisely confined the mineralization age of the Jiaodong gold deposits within the range of 120±5 Ma (Hu et al., 2013; Ma et al., 2017; Deng et al., 2020b), which is consistent with the gold mineralization age in the Liaodong region.

Early Cretaceous gold deposits in Liaodong have similar fluid inclusion characteristics to those in the Jiaodong Peninsula, mainly comprising H_2O-NaCl two-phase and CO_2-bearing inclusions. The mineralization temperature mainly ranges between 200–350°C, and fluid salinity is mostly between 2 wt.% and 15 wt.% NaCl equiv. The ore-forming fluids belong to the H_2O-NaCl-CO_2 hydrothermal system (Figure 6a) (Fan et al., 2016; Deng et al., 2022). Some high-salinity fluid inclusions have been identified from the Liaodong gold deposits (Figure 6a), reflecting characteristics of magmatic hydrothermal fluids. The dominant mechanism for gold precipitation involves either immiscibility or mixing between high-salinity magmatic hydrothermal fluids and low-salinity meteoric water. Hydrogen and oxygen isotopic compositions of gold deposits from both Liaodong and Jiaodong are broadly similar, mainly overlapping with initial magmatic water (Figure 6b), further indicating that the ore-forming fluids were mainly derived from magmatic water, with some involvement of meteoric water. Sulfur isotope δ^{34}S values in the Jiaodong gold deposits are relatively concentrated, mostly between +6‰ and +10‰ (Mao et al., 2008; Li et al., 2018; Feng et al., 2018; Deng et al., 2020b), whereas in the Liaodong gold deposits, δ^{34}S values are more dispersed, ranging from −9.0‰ to +17‰, due to the strong water-rock interaction between the ore-forming fluids and the surrounding rocks (Liaohe Group metamorphic rocks), but still encompassing the δ^{34}S range of the Jiaodong gold deposits. In summary, the ore-forming fluids of gold deposits in both the Liaodong and Jiaodong areas are predominantly of magmatic origin, with some incorporation of meteoric water and exhibiting varying degrees of exchange with the crustal rocks. These characteristics further suggest that gold mineralization in the Liaodong and Jiaodong areas occurred under similar Early Cretaceous tectonic and magmatic settings, characterized by instantaneous explosive mineralization. They have similar mineralization characteristics and temperature-pressure-composition of the ore-forming fluids.

4.4 Metallogenic model of the Liaodong gold deposits

Gold mineralization in the Liaodong region mainly occurred in the Early Cretaceous, and was controlled by fault structures and characterized by intense silicification and sericitization. The C-H-O isotopic compositions of fluid inclusions and sulfide *in-situ* S isotopic compositions indicate that the ore-forming fluids for both quartz vein-type and altered rock-type gold deposits in Liaodong were mainly originated from dehydration of contemporaneous magmas, mixed with meteoric water leaching ore materials from the surrounding rocks (Xu et al., 2020; Wang C Y et al., 2021). Pyrite Sr-Nd-Pb isotopes and *in-situ* S-Fe isotopes reveal that the metal elements such as gold were mainly derived from Early Cretaceous magmatism. The Liaodong gold deposits were formed by mixing of magmatic water and meteoric water that leached ore elements from surrounding rocks,

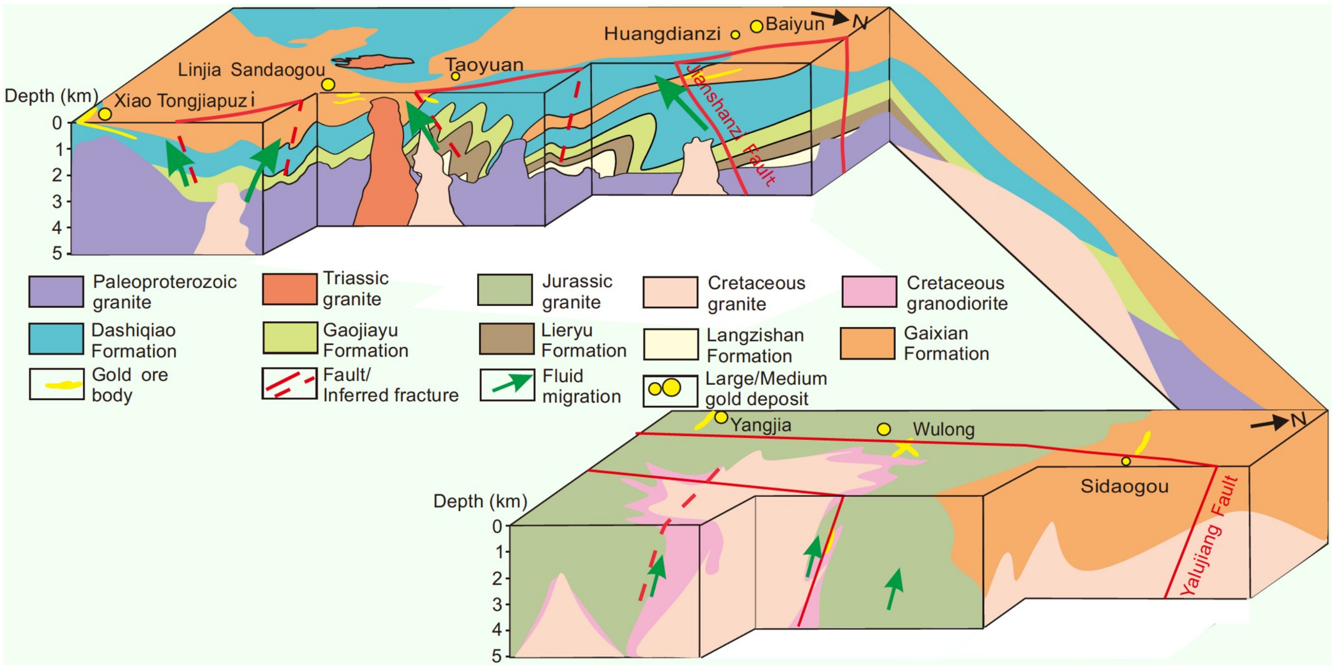

Figure 5 Early Cretaceous tectonism-magmatism-mineralization shallow profile (<5 km) in Qingchengzi and Wulong, Liaodong peninsula.

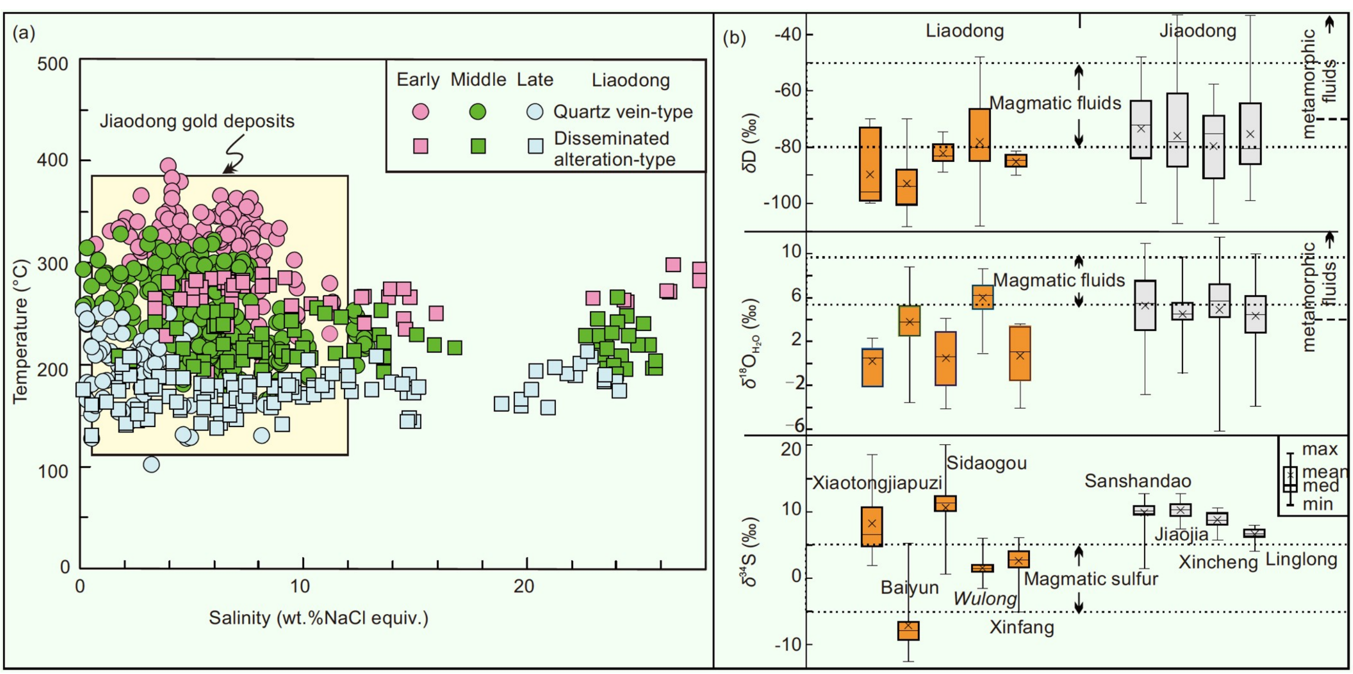

Figure 6 (a) Plot of homogenization temperature and salinity of fluid inclusions from Early Cretaceous Liaodong gold deposits; (b) Comparisons of H-O and pyrite S isotopes between Early Cretaceous Liaodong and Jiaodong gold deposits (modified from Fan et al., 2016 and Deng et al., 2022).

intensive water-rock interaction, and precipitation in favorable structural locations (Xu et al., 2020). Therefore, intensive Early Cretaceous magmatism and extensional tectonics associated with the destruction of the North China Craton were the primary controlling factors for gold mineralization in the Liaodong region and even the eastern part of the craton. Multidisciplinary comprehensive studies have shown that the destruction of the North China Craton and its associated intense tectonic-magmatic-mineralization activities resulted from the subduction of the Paleo-Pacific Plate (Zhu R X et al., 2017; Wu et al., 2019). The spatiotemporal distribution of magmatism and tectonic features in the eastern part of the North China Craton reveals that the subduction process of the Paleo-Pacific Plate toward the East Asian continent during Late Mesozoic time (Zhu and Xu, 2019) is characterized by low-angle subduction in the Jurassic followed by rollback and retreat of the subduction zone in the Early Cretaceous. It was the rollback of the Early Cretaceous subducting plate that led to the destruction of the North China Craton and the associated extensional tectonism-magmatism-gold mineralization geodynamic processes.

Combining regional geological data, we propose the following mineralization model for gold deposits in the Liaodong region and the eastern part of the North China Craton. Since the Late Jurassic-Early Cretaceous, continuous retreat of the subduction zone of the Paleo-Pacific Plate has caused intensive extension in the eastern part of the craton, forming extensional basins and widespread metamorphic core complexes. The rollback of the Pacific Plate induced an unstable mantle flow system, increasing the melt-fluid content in the upper mantle and significantly reducing the lithospheric viscosity, with intensive melt-fluid metasomatism in the ancient lithospheric mantle beneath the eastern North China Craton. At the same time, these processes caused the formation of extensive mantle-derived magmas and fluids in the eastern part of the craton. The crustal materials were partially melted by heating from the upwelling asthenosphere and the mantle-derived magmas at crustal levels, forming felsic magmas. These magmas and deep fluids, carrying part of ore-forming materials, rose along deep faults to different crustal depths, forming complex volcanic and intrusive rocks. Magmatic fluids, formed by dehydration of magmas after crystallization differentiation at shallow crust levels and mixed with meteoric water leaching ore materials from the widely percolated surrounding rocks, formed gold-rich ore-forming fluids. When the ore-forming fluids continued to rise into the shallow fault structural system, rapid boiling/mixing, due to changes in temperature, pressure, and other conditions, caused the precipitation of ore elements such as gold (Figure 7). In our scenario, the Early Cretaceous gold deposits in Liaodong were unlikely to be orogenic but closely related to the destruction of the craton, constituting "Decratonic Gold Deposits" or "Jiaodong-type Gold Deposits."

5. Prospecting potential prediction and breakthrough directions

5.1 Resource potential prediction in typical goldfield of Liaodong

Based on the geodynamical background of gold mineralization and the metallogenic model of deposits in the Liaodong region, a three-dimensional model of the ore-forming geological body in Liaodong has been constructed using geological big data (including geology, geophysics, geochemistry, remote sensing, and supplementary exploration data from typical deposits), artificial intelligence methods (including Random Forest, PU-Learning and other machine learning algorithms), and 2D/3D/4D GIS technology. On this basis, geological big data mining, extraction of three-dimensional exploration variables (including structural and lithological prospecting information as well as density, magnetization, and resistivity ore-related anomaly information), and integrated fusion research were carried out for the Wulong and Qingchengzi goldfields using self-developed Geo-series software (Geosift, Geostatck, GeoPro, GeoSIM, and GeoCube3.0). A new method for delineating favorable prospecting targets and estimating resource potential has been proposed.

(i) Wulong goldfield. Based on the 1:10,000 geological and mineral map, the 1:1000 middle section map, and the borehole database of the Wulong goldfield, models of faults, intrusions, dikes, and ore bodies in the core area of the Wulong goldfield were established using the SKU-GOCAD18.0 software. The Geo-sift software was used to obtain a 1:50,000 gravity-magnetic three-dimensional model of the ore-forming geological body. On this basis, Model Vision software developed by Encom, Australia, was used for a two-and-a-half-degree interpretation of gravity and magnetism, dividing deep geological structures into multiple continuous geological units. Then, UBC-GIF software was used to obtain three-dimensional ore-forming geological body modeling and uncertainty analysis under forward modeling constraints of the Loop3D dataset (depth 5.0 km) of geo-electric profiles. Based on the above three-dimensional models and exploration variable extraction, density, magnetization, resistivity, and their combined variables were interpolated using DSI in the SKUA-GOCAD18.0 software, constructing three-dimensional density inversion models, magnetization inversion models, and resistivity inversion models. Finally, the favorable prospecting target areas in the Wulong goldfields were delineated using the enhanced evidence weight method module of the self-developed quantitative resource prediction and evaluation software GeoCube3.0 (Wang G et al., 2021). Based on this, the gold enrichment-volume (C-V) multi-fractal method was used to divide the Wulong goldfield into three levels (Figure 8a, 8b, 8c). Among them, the first-level target area (Figure 8d) was further divided into Grade A (A-1, A-2, and A-3), Grade B (B-1, B-21, B-3, B-4, B-5, and B-6), and Grade C target areas. Based on the gold content estimation of industrial reserve estimation block units (Wang G et al., 2021), it is estimated that the gold reserves exceed 1000 tons at depths less than 2500 m, with the cumulative resource reserves of the Wulong goldfield exceeding 500 tons.

(ii) Qingchengzi goldfield. Based on the geological and mineral big data of the Qingchengzi goldfield, a preliminary model of faults, intrusions, and ore bodies in the core area of the Qingchengzi goldfield was established using the SKU-

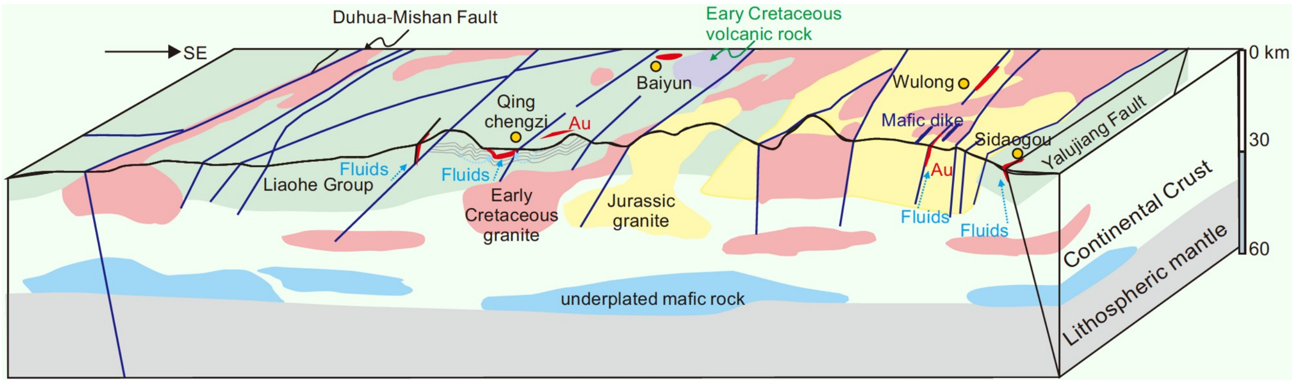

Figure 7 Metallogenic model of Early Cretaceous gold deposits in the Liaodong peninsula.

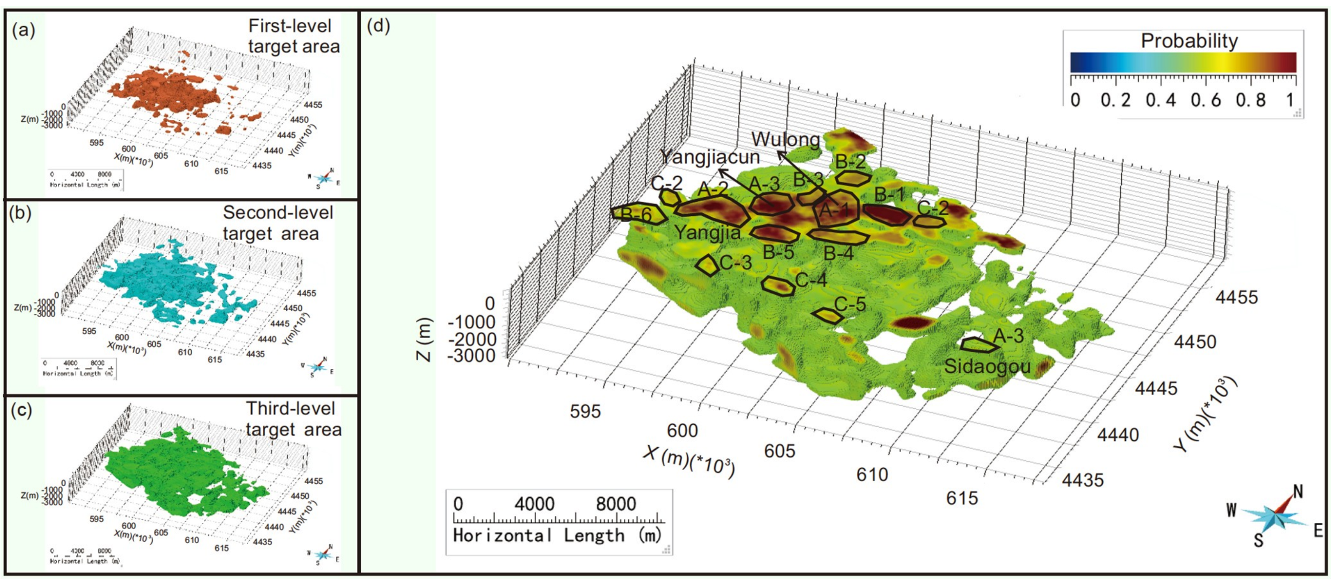

Figure 8 Optimal selection of prospecting targets in the Wulong goldfield based on three-tier (C-V fractal) classification.

GOCAD18.0 software. A multi-parameter 3D spatial information fusion study was conducted, including strata, intrusions, fault buffer zones, dikes, density, magnetization, and resistivity. A three-dimensional model of ore-forming geological body was constructed according to the genetic model of gold deposit and prospecting model. Using the above-mentioned Geo-series geoscience software, an integrated study of exploration variables in the goldfield was carried out. Using 3D RF and 3D PU-Learning methods and their software modules, five prospecting target areas were identified: Baiyun NW section, Huangdianzi NE and SW sections, Xiaotongjiapuzi deep section, and Linjia Sandaogou-Taoyuan deep section (Figure 9). Based on explicit modeling of the Qingchengzi gold deposit (aided by mine tunnel engineering datasets), the number of three-dimensional block units covering industrial ore bodies was obtained, and the gold content of block units was estimated according to the industrial reserves (Wang G et al., 2021). The number of three-dimensional block units outside the known gold orebodies (first-tier target areas) was counted. The first-tier target areas have similar exploration variables and combinations and higher values of Bayesian posterior probability compared to known orebodies. The reserves in the target areas was calculated based on the product of the number of block units and the gold content values. The gold resource at a depth of 500–2500 m in the Qingchengzi goldfield was estimated to reach 1619 tons using GeoCube3.0 and SKUA-GOCAD software.

5.2 Prospecting indicators

The geological characteristics and genesis of the known gold deposits in the Liaodong region have provided clear prospecting indicators. One indicator is the development of the middle Early Cretaceous (120–125 Ma) mantle-derived mafic intrusions, specifically diorite, diabase and lamprophyre that occur as dikes and locally as stocks. The extent of these mafic intrusions is often proportional to the degree of

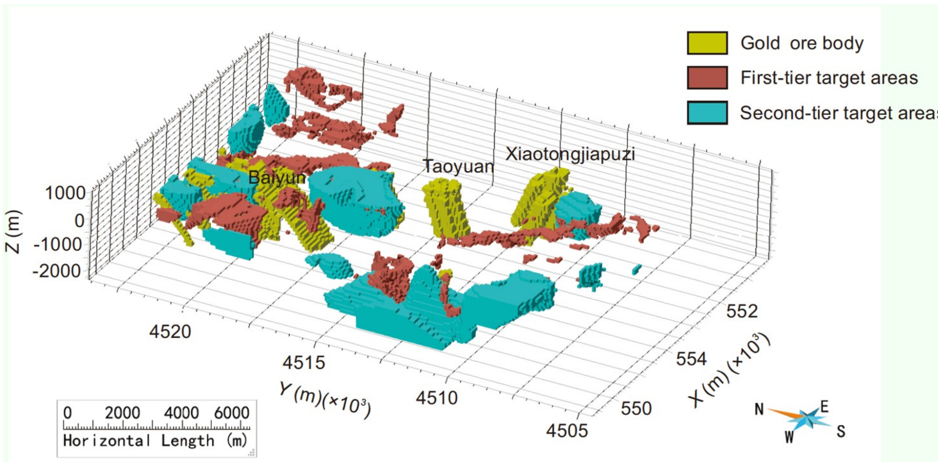

Figure 9 Three-dimensional model of prospecting targets in the Qingchengzi goldfield.

gold mineralization, making them the most favorable sites for locating altered rock-type or quartz vein-type gold deposits. The second indicator is the crust-mantle mixed-source intermediate-acidic intrusions in the Early Cretaceous (125–130 Ma), mainly granodiorite. These intermediate-acidic intrusions are also favorable areas for gold enrichment. The third indicator is the regional development of Late Jurassic crustal granites, often accompanying gold mineralization belts, forming an important petrological background for gold mineralization. The fourth indicator is the Early Cretaceous extensional structures developing during the mineralization period, including normal faults, extensional detachment zones, interlayer sliding zones, and faults along the boundaries of intrusions. Brittle-ductile extensional structures are the most favorable sites for gold mineralization.

It is worth noting that the spatial overlap of the three phases of intrusion with Early Cretaceous extensional structures is the most favorable gold mineralization area in the Liaodong region. The intensity of these three phases of magmatism and extensional activities is directly proportional to the degree of gold mineralization. The mantle-derived magmatism and extensional activity in the Early Cretaceous are necessary conditions for gold mineralization in Liaodong, while the Early Cretaceous and Late Jurassic magmatism is sufficient conditions. Gold mineralization was closely associated with Early Cretaceous mantle-derived magmatism and extensional activity, while Early Cretaceous and Late Jurassic crustal-derived magmatism often developed around or deep within gold deposits.

The Liaohe Group, composed of the Langzishan, Lieryu, Gaojiayu, Dashiqiao, and Gaixian Formations, sequentially composed of dolomites, volcanic rocks, carbonate rocks, and mudstones from bottom to top (Luo et al., 2004; Li et al., 2005). The Gaixian Formation of the Liaohe Group, with its massive mudstone and sandstone deposits, has the lowest degree of metamorphism and the highest gold content (Cui et al., 2022); it is also the most altered formation, making the Gaixian Formation the most favorable stratigraphic level for locating altered rock-type gold deposits in Liaodong.

5.3 Breakthrough directions in prospecting

Although it is still uncertain whether the Liaodong gold deposits have multi-layer enrichment characteristics at different depths similar to those of the Jiaodong gold deposits, the Liaodong and Jiaodong areas have similar geological evolutionary history, geological characteristics of gold deposits, mineralization processes and geological settings. Recent multidisciplinary comprehensive exploration data also indicate the immense potential of gold resources in Liaodong, which should be one of China's most important strategic gold resource replacement bases. Suggestions for recent key research and breakthrough directions in prospecting are as follows:

(i) Deep/surround parts of known gold deposits. Apart from the Wulong gold deposit, most gold deposits in the Liaodong area have been explored and mined to depths of less than 500 m. However, each gold orefield in Liaodong widely contains Early Cretaceous intermediate-acidic dikes and contemporaneous ore-controlling faults closely associated with gold mineralization. The shallow parts of the deposits developed with the intensive alteration of the wall rocks (such as silicification, sericitization, chloritization, etc.), characterized by strong alteration with less noticeable variation. Geophysical exploration also indicates that the known auriferous veins extend significantly into deeper and peripheral parts. Deep drilling in the Qingchengzi goldfield has revealed the orebody (vein 130) at a depth of 1692 m, which is the deepest one known in Liaodong. Drilling in the Wulong gold deposit has found gold-bearing quartz veins at a depth of 1500 m, with a thickness of 3.7 m and a grade of

5.74 g/t. Regional geological studies also show that veins in the known goldfields extend significantly into the periphery and side parts, showing continuous development along structures, accompanied by alteration of the surrounding rocks and gold mineralization. For instance, in the Wulong goldfield, hundreds of gold-bearing quartz veins have been identified, which show similar ore-controlling structures, alteration of the surrounding rocks, and mineralization to the well-known goldfield, but exploration of these gold-bearing quartz veins is currently still at an initial stage. In the Qingchengzi goldfield, the known mineralized alteration zone of the Baiyun gold deposit extends westward from Lijiapu to Fengjiapuzi. At the Fengjiapuzi artisanal mining site, gold-bearing quartz veins were found with a grade of 8.97 g/t, and the width of alteration zone reaches 50–60 m. Controlled-source electromagnetic exploration has revealed a low-resistance anomaly zone extending over 4000 m in strike and extending down to 400–1500 m in dip, coinciding with the surface-observed alteration zone. These findings indicate that both the deep and peripheral parts of known goldfields in Liaodong hold significant prospecting potential.

(ii) Altered rock-type gold deposits along large faults. The Liaodong region has a regional structural framework similar to that of the Jiaodong region, with a series of large NNE-trending faults and adjacent secondary NS-trending faults. In the Jiaodong region, several large and super-large altered rock-type gold deposits have developed along NNE-trending main faults, such as the Sanshandao, Jiaojia, and Zhao-Ping faults. However, super-large gold deposits have not yet been found along similar NNE-trending large faults in the Liaodong region. In terms of characteristics of fault structure, the NNE-trending faults in the Liaodong region are very similar to the ore-controlling faults in the Jiaodong region. They often exhibit progressive activity from early ductile to late brittle phases, developing fracture zones and closely associated gold mineralization with alterations such as silicification and sericitization (with some showing obvious gold mineralization) and are characterized by obvious low resistivity anomalies and positive magnetic anomalies. For example, a newly discovered fractured altered rock-type gold orebody in the NNE-trending Jixingou fault zone in the Wulong goldfield will be verified by drilling and needs further in-depth exploration. In the Qingchengzi goldfield, the Jianshanzi fault controls the distribution of major gold deposits. Existing drilling data indicate that a gold mineralization zone developed within the fault reaches over 100 m in thickness and extends down-dip for 1100–1600 m, with local gold grades reaching 2.72 g/t and an average gold grade of 0.19 g/t.

The NNE-trending Yalu River fault zone, extending over 700 km along the China-North Korea border, is a significant ore-controlling structure in the Liaodong region, controlling the development of various types of gold deposits. The altered rock-type gold deposits discovered along this large fault zone include the Shawogou, Qiuguobi, Xinfang peripheral gold deposits. The Dadonggou gold deposit in Gaizhou also formed within the sericite-quartz schist layer of the Gaixian Formation of the Liaohe Group (Li et al., 2019), which is an superlarge gold deposit. The host rocks of these gold deposits are the Gaixian Formation of the Liaohe Group. In addition, altered rock-type and quartz vein-type superimposed gold deposits have been discovered along the Yalu River fault zone, represented by the Xiahekou, Daguling, and Xinfang gold deposits, of which the Xinfang gold deposit has already become a large gold deposit. The host rocks of the Xiahekou, Daguling and Xinfang gold deposits are the Gaojiayu, Gaojiayu and Dashiqiao Formations of the Liaohe Group, and the Archean Anshan Group. Along the Yalu River fault zone and its adjacent secondary faults, a series of quartz vein-type gold deposits or mineralization points have also been discovered, including the Miaotaizi, Nanlingwai, Gongdonggou, and Laobianqiang gold deposits, whose host rocks are all Late Mesozoic granites, also showing significant prospecting potential. These preliminary studies have indicated that the fractured alteration zones and quartz vein-type gold deposits within the Yalu River fault zone in the Liaodong region will be an important breakthrough for future prospecting, with a potential to add a thousand ton of exploitable gold reserves.

6. Conclusions

Gold deposits in the Liaodong region were mainly formed in the Early Cretaceous, controlled by fault structures and characterized by intensive silicification and sericitization. The gold mineralization was closely related to Early Cretaceous magmatism associated with lithospheric thinning and the craton destruction in the eastern North China Craton. Gold deposits in both the Liaodong and Jiaodong regions have very similar regional geological evolution, mineralization ages, mineralization process, etc., and thus can be termed as “the Decratonic Gold Deposits” or “the Jiaodong-type Gold Deposits”, which were closely related to craton destruction. Studies of Mesozoic magmatic-tectonic evolution and metallogenesis, deep-shallow integrated geophysical exploration, and big data AI resource prediction indicate that the Liaodong region holds an immense potential for gold resources, making it another significant “thousand-ton class” strategic base of gold resources in China. Based on recent research and exploration results, in this paper we propose that the Yalu River fault zone and its surrounding areas are key regions for future gold exploration, with the periphery and deep parts of known goldfield being important prospecting targets.

Acknowledgements *Thanks to CAS Academician Qingyun DI from the Institute of Geology and Geophysics, Chinese Academy of Sciences, Professor Deming SHA from the Shenyang Geological Survey Center, China Geological Survey, and Professor Fuxing LIU from the Liaoning Nonferrous Geology 103 Team Co., Ltd. for their discussions and constructive suggestions. Thanks to Professors Shuwen DONG of Nanjing University and Guochun ZHAO of the University of Hong Kong for their careful revision and suggestion. We also thanks to three anonymous reviewers for their valuable suggestions and careful revisions. This paper has employed the English translation and polishing functions of ChatGPT. This work was supported by the National Natural Science Foundation of China (Grant No. 42288201), and the National Key Research & Development Program of the Ministry of Science and Technology of China (Grant No. 2016YFC0600109).*

Conflict of interest The authors declare that they have no conflict of interest.

References

Chen L. 2010. Concordant structural variations from the surface to the base of the upper mantle in the North China Craton and its tectonic implications. Lithos, 120: 96–115

Cui W L, Guo J H, Huang G Y, Wang Z C, Liu Y H, Yang J H. 2022. Gold mobilization during prograde metamorphism of clastic sedimentary rocks: An example from the Liaohe Group in the Jiao-Liao-Ji Belt, North China Craton. Ore Geol Rev, 140: 104624

Deng J, Liu X F, Wang Q F, Pan R G. 2015. Origin of the Jiaodong-type Xinli gold deposit, Jiaodong Peninsula, China: Constraints from fluid inclusion and C–D–O–S–Sr isotope compositions. Ore Geol Rev, 65: 674–686

Deng J, Qiu K F, Wang Q F, Goldfarb R J, Yang L Q, Zi J W, Geng J Z, Ma Y. 2020b. *In-situ* dating of hydrothermal monazite and implications on the geodynamic controls of ore formation in the Jiaodong gold province, eastern China. Econ Geol, 115: 671–685

Deng J, Wang Q F, Liu X F, Zhang L, Yang L Q, Yang L, Qiu K F, Guo L N, Liang Y Y, Ma Y. 2022. The formation of the Jiaodong gold province. Acta Geol Sin-Engl Ed, 96: 1801–1820

Deng J, Wang Q, Zhang L, Xue S, Liu X, Yang L, Yang L, Qiu K, Liang Y. 2023. Metallogenetic model of Jiaodong-type gold deposits, eastern China. Sci China Earth Sci, 66: 2287–2310

Deng J, Yang L Q, Groves D I, Zhang L, Qiu K F, Wang Q F. 2020a. An integrated mineral system model for the gold deposits of the giant Jiaodong province, eastern China. Earth-Sci Rev, 208: 103274

Di Q Y, Xue G Q, Lei D, Zeng Q D, Fu C M, An Z G. 2021. Summary oftechnologyforacomprehensivegeophysicalexploration of gold-mineinNorthChinaCraton. Sci China Earth Sci, 64: 1524–1536

Di Q Y, Xue G Q, Zeng Q D, Wang Z X, An Z G, Lei D. 2020. Magnetotelluric exploration of deep-seated gold deposits in the Qingchengzi orefield, Eastern Liaoning (China), using a SEP system. Ore Geol Rev, 122: 103501

Dong W Y, Xu T, Ai Y S, Fan E B, Li L, Hou J. 2022. The boundary between the North China Craton and the Central Asian Orogenic Belt in NE China: Seismic evidence from receiver function imaging. J Asian Earth Sci, 237: 105360

Fan H R, Feng K, Li X H, Hu F F, Yang K F. 2016. Mesozoic gold mineralization in the Jiaodong and Korean peninsulas (in Chinese). Acta Petrol Sin, 32: 325–3238

Fan H R, Lan T G, Li X H, Santosh M, Yang K F, Hu F F, Feng K, Hu H L, Peng H W, Zhang Y W. 2021. Conditions andprocessesleadingtolarge-scalegolddepositionintheJiaodongprovince,easternChina. Sci China Earth Sci, 64: 1504–1523

Feng H X, Shen P, Zhu R X, Ma G, Li C H, Li J P. 2020. SIMS U-Pb dating of vein-hosted hydrothermal rutile and carbon isotope of fluids in the Wulong lode gold deposit, NE China: Linking gold mineralization with craton destruction. Ore Geol Rev, 127: 103838

Feng K, Fan H R, Hu F F, Yang K F, Liu X, Shangguan Y N, Cai Y C, Jiang P. 2018. Involvement of anomalously As-Au-rich fluids in the mineralization of the Heilan'gou gold deposit, Jiaodong, China: Evidence from trace element mapping and *in-situ* sulfur isotope composition. J Asian Earth Sci, 160: 304–321

Gebre-Mariam M, Hagemann S G, Groves D I. 1995. A classification scheme for epigenetic Archaean lode-gold deposits. Mineral Depos, 30: 408–410

Goldfarb R J, Groves D I, Gardoll S. 2001. Orogenic gold and geologic time: A global synthesis. Ore Geol Rev, 18: 1–75

Goldfarb R J, Groves D I. 2015. Orogenic gold: Common or evolving fluid and metal sources through time. Lithos, 233: 2–26

Groves D I, Goldfarb R J, Gebre-Mariam M, Hagemann S G, Robert F. 1998. Orogenic gold deposits: A proposed classification in the context of their crustal distribution and relationship to other gold deposit types. Ore Geol Rev, 13: 7–27

Hu F F, Fan H R, Jiang X H, Li X C, Yang K F, Mernagh T. 2013. Fluid inclusions at different depths in the Sanshandao gold deposit, Jiaodong Peninsula, China. Geofluids, 13: 528–541

Jiang N, Guo J H, Zhai M G, Zhang S Q. 2010. ~2.7 Ga crust growth in the North China craton. Precambrian Res, 179: 37–49

Li H, Li Y, Ma S, Wang P, Wei W, Fan J H, Zheng J, Liu H J. 2019. LA-ICP-MS zircon U-Pb age and petrochemical characteristics of magmatite from the Dadonggou gold deposit in east Liaoning (in Chinese). Geol Bull China, 38: 1543–1555

Li S Z, Zhao G C, Sun M, Han Z, Luo Y, Hao D, Xia X. 2005. Deformation history of the Paleoproterozoic Liaohe assemblage in the eastern block of the North China Craton. J Asian Earth Sci, 24: 659–674

Li X H, Fan H R, Yang K F, Hollings P, Liu X, Hu F F, Cai Y C. 2018. Pyrite textures and compositions from the Zhuangzi Au deposit, southeastern North China craton: Implication for ore-forming processes. Contrib Mineral Petrol, 173: 73

Lin W, Faure M, Monie P, Scharer U, Panis D. 2008. Mesozoic extensional tectonics in eastern Asia: The South Liaodong Peninsula metamorphic core complex (NE China). J Geol, 116: 134–154

Lin W, Monié P, Faure M, Schärer U, Shi Y H, Breton N L, Wang Q C. 2011. Cooling paths of the NE China crust during the Mesozoic extensional tectonics: Example from the south-Liaodong peninsula metamorphic core complex. J Asian Earth Sci, 42: 1048–1065

Liu J L, Ji M, Shen L, Guan H M, Davis G A. 2011. Early Cretaceous extensional structures in the Liaodong Peninsula: Structural associations, geochronological constraints and regional tectonic implications. Sci China Earth Sci, 54: 823–842

Liu J, Li T G, Duan C. 2018. Geochronology and isotopic geochemistry characteristics of the Maoling large gold deposit, Liaodong Province, China (in Chinese). Geol Bull China, 37: 1325–1337

Liu J L, Shen L, Ji M, Guan H, Zhang Z, Zhao Z. 2013. The Liaonan/Wanfu metamorphic core complexes in the Liaodong Peninsula: Two stages of exhumation and constraints on the destruction of the North China Craton. Tectonics, 32: 1121–1141

Liu J L, Zhang L J, Wang S L, Li T G, Yang Y, Liu F X, Li S H, Duan C. 2019. Formation of the Wulong gold deposit, Liaodong gold Province, NE China: Constraints from zircon U-Pb age, sericite Ar-Ar age, and H–O–S–He isotopes. Ore Geol Rev, 109: 130–143

Luo Y, Sun M, Zhao G C, Li S Z, Xu P, Ye K, Xia X. 2004. LA-ICP-MS U-Pb zircon ages of the Liaohe Group in the Eastern Block of the North China Craton: Constraints on the evolution of the Jiao-Liao-Ji Belt. Precambrian Res, 134: 349–371

Ma L X, Xu T, Ai Y S, Yang J H, Yang Y J, Fan E B, Li L, Hou J, Dong W Y. 2022. Hot Lithosphere beneath the northeastern North China Craton detected by ambient noise tomography. Tectonophysics, 839: 229551

Ma W D, Fan H R, Liu X, Pirajno F, Hu F F, Yang K F, Yang Y H, Xu W G, Jiang P. 2017. Geochronological framework of the Xiadian gold deposit in the Jiaodong province, China: Implications for the timing of gold mineralization. Ore Geol Rev, 86: 196–211

Mao J W, Liu P, Goldfarb R J, Goryachev N A, Pirajno F, Zheng W, Zhou

M F, Zhao C, Xie G Q, Yuan S D, Liu M. 2021. Cretaceous large-scale metal accumulation triggered by post-subductional large-scale extension, East Asia. Ore Geol Rev, 136: 104270

Mao J W, Wang Y T, Li H M, Pirajno F, Zhang C Q, Wang R T. 2008. The relationship of mantle-derived fluids to gold metallogenesis in the Jiaodong Peninsula: Evidence from D–O–C–S isotope systematics. Ore Geol Rev, 33: 361–381

Mao J W, Xie G Q, Zhang Z H, Li X F, Wang T Y, Zhang C Q, Li Y F. 2005. Mesozoic large-scale metallogenic pulses in North China and corresponding geodynamic settings (in Chinese). Acta Petrol Sin, 21: 169–188

Meng F, Ai Y S, Xu T, Chen L, Wang X, Li L. 2021. Lithospheric structure beneath the boundary region of North China Craton and Xing Meng Orogenic Belt from S-receiver function analysis. Tectonophysics, 818: 229067

Miao L C, Luo Z K, Huang J Z, Guan K, Wang G L, Mcnaughton J N, Groves I D. 1997. Zircon sensitive high resolution ion microprobe (SHRIMP) study of granitoid intrusions in the Zhaoye gold belt of Shandong province and its implication. Sci China Ser D-Earth Sci, 40: 361–369

Phillips G N, Powell R. 2010. Formation of gold deposits: A metamorphic devolatilization model. J Metamorph Geol, 28: 689–718

Sun F Y, Shi Z L. 1995. The relationship between lamprophyres and some hydrothermal deposits: Implications for a differentiation model of mantle-derived C-H-O fluids (in Chinese). Contributions to Geology and Mineral Resources Research, 2: 72–81

Sun G T, Zeng Q D, Li T Y, Li A, Wang E Y, Xiang C S, Wang Y B, Chen P W, Yu B. 2019. Ore genesis of the Baiyun gold deposit in Liaoning province, NE China: Constraints from fluid inclusions and zircon U-Pb ages. Arab J Geosci, 12: 299

Sun G T, Zeng Q D, Zhou L L, Philip Hollis S, Zhou J X, Chen K. 2022. Mechanisms for invisible gold enrichment in the Liaodong Peninsula, NE China: *In situ* evidence from the Xiaotongjiapuzi deposit. Gondwana Res, 103: 276–296

Sun G T, Zeng Q D, Zhou L L, Wang Y B, Chen P W. 2020. Trace element contents and *in situ* sulfur isotope analyses of pyrite in the Baiyun gold deposit, NE China: Implication for the genesis of intrusion-related gold deposits. Ore Geol Rev, 118: 103330

Sun J F, Zhang J H, Yang J H, Zhu Y S, Chen J Y, Ling-Hu M M. 2021. Multi-stage Jurassic magmatism in the Liaodong Peninsula: Constraints on crustal evolution beneath the eastern North China Craton. Lithos, 402-403: 105897

Tomkins A G. 2010. Windows of metamorphic sulfur liberation in the crust: Implications for gold deposit genesis. Geochim Cosmochim Acta, 74: 3246–3259

Wang C Y, Wei B, Tan W, Wang Z, Zeng Q. 2021. The distribution, characteristics and fluid sources of lode gold deposits: An overview. Sci China Earth Sci, 64: 1463–1480

Wang G, Zhang Z, Li R, Li J, Sha D, Zeng Q, Pang Z, Li D, Huang L. 2021. Resource prediction and assessment based on 3D/4D big data modeling and deep integration in key ore districts of North China. Sci China Earth Sci, 64: 1590–1606

Wu F Y, Lin J Q, Wilde S A, Zhang X O, Yang J H. 2005a. Nature and significance of the Early Cretaceous giant igneous event in Eastern China. Earth Planet Sci Lett, 233: 103–119

Wu F Y, Yang J H, Wilde S A, Zhang X O. 2005b. Geochronology, petrogenesis and tectonic implications of Jurassic granites in the Liaodong Peninsula, NE China. Chem Geol, 221: 127–156

Wu F Y, Yang J H, Xu Y G, Wilde S A, Walker R J. 2019. Destruction of the North China Craton in the Mesozoic. Annu Rev Earth Planet Sci, 47: 173–195

Xiao S Y, Zhu G, Zhang S, Liu C, Su N, Yin H, Wu X D, Li Y J. 2018. Structural processes and dike emplacement mechanism in the Wulong gold field, eastern Liaoning (in Chinese). Chin Sci Bull, 63: 3022–3036

Xie T T, Xu T, Ai Y S, Zeng Q D, Zhang W, Zheng F. 2021. Imaging the shallow crustal velocity structure of the Qingchengzi ore field on the Liaodong Peninsula, China, with a short-period dense array using ambient noise tomography. Tectonophysics, 813: 228913

Xu L, Yang J H, Zeng Q D, Xie L W, Zhu Y S, Li R, Li B. 2020. Pyrite Rb-Sr, Sm-Nd and Fe isotopic constraints on the age and genesis of the Qingchengzi Pb-Zn deposits, northeastern China. Ore Geol Rev, 117: 103324

Yan D P, Kong R, Dong X, Qiu L, Liu H. 2021. Late Jurassic-Early Cretaceous tectonic switching in Liaodong Peninsula of the North China Craton and the implications for gold mineralisation. Sci China Earth Sci, 64: 1537–1556

Yang J H, Sun J F, Zhang J H, Wilde S A. 2012. Petrogenesis of Late Triassic intrusive rocks in the northern Liaodong Peninsula related to decratonization of the North China Craton: Zircon U-Pb age and Hf-O isotope evidence. Lithos, 153: 108–128

Yang J H, Wu F Y, Chung S L, Lo C H, Wilde S A, Davis G A. 2007. Rapid exhumation and cooling of the Liaonan metamorphic core complex: Inferences from $^{40}Ar/^{39}Ar$ thermochronology and implications for Late Mesozoic extension in the eastern North China Craton. GSA Bull, 119: 1405–1414

Yang J H, Wu F Y, Chung S L, Wilde S A, Chu M F, Lo C H, Song B. 2005. Petrogenesis of Early Cretaceous intrusions in the Sulu ultrahigh-pressure orogenic belt, east China and their relationship to lithospheric thinning. Chem Geol, 222: 200–231

Yang J H, Wu F Y, Wilde S A. 2003. A review of the geodynamic setting of large-scale Late Mesozoic gold mineralization in the North China Craton: An association with lithospheric thinning. Ore Geol Rev, 23: 125–152

Yang J H, Wu F Y. 2009. Triassic magmatism and its relation to decratonization in the Eastern North China Craton. Sci China Ser D-Earth Sci, 52: 1319–1330

Yang J H, Xu L, Sun J F, Zeng Q, Zhao Y N, Wang H, Zhu Y S. 2021. Geodynamics of decratonization and related magmatism and mineralization in the North China Craton. Sci China Earth Sci, 64: 1409–1427

Yang J H, Zhou X H. 2001. Rb-Sr, Sm-Nd, and Pb isotope systematics of pyrite: Implications for the age and genesis of lode gold deposits. Geology, 29: 711–714

Yu B, Zeng Q D, Frimmel H E, Qiu H C, Li Q L, Yang J H, Wang Y B, Zhou L L, Chen P W, Li J P. 2020. The 127 Ma gold mineralization in the Wulong deposit, Liaodong Peninsula, China: Constraints from molybdenite Re-Os, monazite U-Th-Pb, and zircon U-Pb geochronology. Ore Geol Rev, 121: 103542

Yu B, Zeng Q D, Frimmel H E, Yang J H, Zhou L L, Drakou F, Mcclenaghan S H, Wang Y B, Wang R L. 2022. The genesis of Xindian gold deposit, Liaodong Peninsula, NE China: Constraints from zircon U-Pb ages, S-Pb isotopes, and pyrite trace element chemistry. Resour Geol, 72: e12303

Yu B, Zeng Q D, Frimmel H E, Wang Y, Guo W, Sun G, Zhou T, Li J. 2018. Genesis of the Wulong gold deposit, northeastern North China Craton: Constraints from fluid inclusions, H-O-S-Pb isotopes, and pyrite trace element concentrations. Ore Geol Rev, 102: 313–337

Yu C, Zhong R C, Tomkins A G, Cui H, Chen Y J. 2024. Expanding the metamorphic devolatilization model: Komatiites as a source for orogenic gold deposits in high-grade metamorphic rocks. Geology, 52: 67–71

Yu G, Yang G, Chen J F, Qu W J, He W. 2005. Re-Os dating of gold-bearing arsenopyrite of the Maoling gold deposit, Liaoning Province, Northeast China and its geological significance. Chin Sci Bull, 50: 1509–1514

Zeng Q D, Chen R Y, Yang J H, Sun G T, Yu B W Y B, Chen P W. 2019. The metallogenic characteristics and exploring ore potential of the gold deposits in eastern Liaoning Province (in Chinese). Acta Petrologica Sin, 35: 1939–1963

Zhang P, Zhao Y, Chai P, Yang H Z, Na F C. 2017. Geochemistry, zircon U-Pb analysis, and biotite $^{40}Ar/^{39}Ar$ geochronology of the Maoling Gold Deposit, Liaodong Rift, NE China. Resour Geol, 67: 426–441

Zhang P, Zhao Y, Kou L L, Yang H Z, Sha D M, Yang Z Z, Zhang J, Yu C. 2022. Genesis of the Xinfang magmatic-hydrothermal gold deposit, Liaodong Peninsula, China: Constraints from pyrite Re-Os isotopes, C,

O, S, Pb, Si, He and Ar isotopes. Ore Geol Rev, 148: 105025
Zhang P, Zhao Y, Kou L L, Yang H Z. 2023. Genesis of the Xinfang gold deposit, Liaodong Peninsula: Constraints from fluid inclusions, H-O-S-Pb isotopes, pyrite trace element concentrations, and chronology. Gondwana Res, 113: 210–231
Zhang Q S, Yang Z S, Liu L D. 1988. Early Crust and Mineral Deposits in the Liaodong Peninsula (in Chinese). Beijing: Geological Publishing House. 218–450
Zhang R Q, Wu Q J, Sun L, He J, Gao Z Y. 2014. Crustal and lithospheric structure of Northeast China from S-wave receiver functions. Earth Planet Sci Lett, 401: 196–205
Zhang S H, Hu G H, Li J F, Xiao C H, Liu X C, Zhang Q Q, Yao X F, Liu F X, Wang W, Chen Z L, Zhang Q. 2020. Ore-controlling structures and metallogenic favorable area prediction in Baiyun-Xiaotongjiabuzi ore concentration area, eastern Liaoning Province (in Chinese). Earth Sci, 45: 3885–3899
Zhang S, Zhu G, Gu C C, Liu C, Li Y J, Zhao T, Wang W. 2017. Discussion on the southeastern boundary location of the Liao-Ji orogenic belt (in Chinese). Chin Sci Bull, 62: 2814–2828
Zhang S, Zhu G, Liu C, Li Y, Su N, Xiao S, Gu C. 2018. Strike-slip motion within the Yalu River Fault Zone, NE Asia: The development of a shear continental margin. Tectonics, 37: 1771–1796
Zhang S, Zhu G, Liu C, Li Y, Su N, Xiao S. 2019. Episodicity of stress state in an overriding plate: Evidence from the Yalu River Fault Zone, East China. Gondwana Res, 71: 150–178
Zhang S, Zhu G, Xiao S Y, Su N, Liu C, Wu X D, Yin H, Li Y J, Lu Y C. 2020. Temporal variations in the dynamic evolution of an overriding plate: Evidence from the Wulong area in the eastern North China Craton, China. GSA Bull, 132: 2023–2042
Zheng F, Xu T, Ai Y S, Yang Y J, Zeng Q D, Yu B, Zhang W, Xie T T. 2022. Metallogenic potential of the Wulong goldfield, Liaodong Peninsula, China revealed by high-resolution ambient noise tomography. Ore Geol Rev, 142: 104704
Zheng Y F, Xu Z, Zhao Z F, Dai L Q. 2018. Mesozoic mafic magmatism in North China: Implications for thinning and destruction of cratonic lithosphere. Sci China Earth Sci, 61: 353–385
Zheng Y F, Zhao Z F, Chen R X. 2019. Ultrahigh-pressure metamorphic rocks in the Dabie-Sulu orogenic belt: Compositional inheritance and metamorphic modification. Geol Soc Lond Spec Publ, 474: 89–132
Zhu G, Liu C, Gu C C, Zhang S, Li Y J, Su N, Xiao S Y. 2018. Oceanic plate subduction history in the western Pacific Ocean: Constraint from late Mesozoic evolution of the Tan-Lu Fault Zone. Sci China Earth Sci, 61: 386–405
Zhu G, Lu Y, Su N, Wu X, Yin H, Zhang S, Xie C, Niu M. 2021. Crustal deformation and dynamics of Early Cretaceous in the North China Craton. Sci China Earth Sci, 64: 1428–1450
Zhu G, Jiang D Z, Zhang B L, Chen Y. 2012. Destruction of the eastern North China Craton in a backarc setting: Evidence from crustal deformation kinematics. Gondwana Res, 22: 86–103
Zhu R X, Chen L, Wu F Y, Liu J L. 2011. Timing, scale and mechanism of the destruction of the North China Craton. Sci China Earth Sci, 54: 789–797
Zhu R X, Fan H R, Li J W, Meng Q R, Li S R, Zeng Q D. 2015. Decratonic gold deposits. Sci China Earth Sci, 58: 1523–1537
Zhu R X, Xu Y G, Zhu G, Zhang H F, Xia Q K, Zheng T Y. 2012. Destruction of the North China Craton. Sci China Earth Sci, 55: 1565–1587
Zhu R X, Xu Y G. 2019. The subduction of the west Pacific plate and the destruction of the North China Craton. Sci China Earth Sci, 62: 1340–1350
Zhu R X, Zhang H F, Zhu G, Meng Q R, Fan H R, Yang J H, Wu F Y, Zhang Z Y, Zheng T Y. 2017. Craton destruction and related resources. Int J Earth Sci-Geol Rund, 106: 2233–2257
Zhu R X, Zhu G, Li J W. 2020. The North China Craton Destruction (in Chinese). Beijing: Science Press. 1–417
Zhu Y S, Yang J H, Sun J F, Wang H. 2017. Zircon Hf-O isotope evidence for recycled oceanic and continental crust in the sources of alkaline rocks. Geology, 45: 407–410

(Editorial handling: Huayong CHEN)